



Highly selective spectral response with enhanced responsivity of n -ZnO / p -Si radial heterojunction nanowire photodiodes

Han-Don Um, Syed Abdul Moiz, Kwang-Tae Park, Jin-Young Jung, Sang-Won Jee, Cheol Hyoun Ahn, Dong Chan Kim, Hyung Koun Cho, Dong-Wook Kim, and Jung-Ho Lee

Citation: [Applied Physics Letters](#) **98**, 033102 (2011); doi: 10.1063/1.3543845

View online: <http://dx.doi.org/10.1063/1.3543845>

View Table of Contents: <http://scitation.aip.org/content/aip/journal/apl/98/3?ver=pdfcov>

Published by the [AIP Publishing](#)

Articles you may be interested in

[p-Si nanowires/ SiO₂/n-ZnO heterojunction photodiodes](#)
Appl. Phys. Lett. **97**, 013503 (2010); 10.1063/1.3462319

[Response to "Comment on 'Deep ultraviolet and near infrared photodiode based on n -ZnO / p -silicon nanowire heterojunction at low temperature'" \[Appl. Phys. Lett.94, 166102 \(2009\)\]](#)
Appl. Phys. Lett. **94**, 166103 (2009); 10.1063/1.3119200

[Comment on "Deep ultraviolet and near infrared photodiode based on n -ZnO / p -silicon nanowire heterojunction at low temperature" \[Appl. Phys. Lett.94, 013503 \(2009\)\]](#)
Appl. Phys. Lett. **94**, 166102 (2009); 10.1063/1.3119197

[Deep ultraviolet and near infrared photodiode based on n -ZnO / p -silicon nanowire heterojunction fabricated at low temperature](#)
Appl. Phys. Lett. **94**, 013503 (2009); 10.1063/1.3064161

[Visible and ultraviolet light alternative photodetector based on ZnO nanowire/ n - Si heterojunction](#)
Appl. Phys. Lett. **93**, 163501 (2008); 10.1063/1.3003877

The image shows the cover of an Applied Physics Reviews journal issue. It features a white cover with a diagram of a device structure and the text 'AIP Applied Physics Reviews'. The background is a blue gradient with a bright light source on the right and several blue spheres of varying sizes on the left.

NEW Special Topic Sections

NOW ONLINE
Lithium Niobate Properties and Applications:
Reviews of Emerging Trends

AIP | Applied Physics Reviews

Highly selective spectral response with enhanced responsivity of n -ZnO/ p -Si radial heterojunction nanowire photodiodes

Han-Don Um,¹ Syed Abdul Moiz,² Kwang-Tae Park,¹ Jin-Young Jung,² Sang-Won Jee,² Cheol Hyoun Ahn,³ Dong Chan Kim,³ Hyung Koun Cho,³ Dong-Wook Kim,^{4,a)} and Jung-Ho Lee^{1,2,a)}

¹Department of Bio-Nano Technology, Hanyang University, Ansan 426-791, South Korea

²Department of Materials and Chemical Engineering, Hanyang University, Ansan 426-791, South Korea

³School of Advanced Materials Science and Engineering, Sungkyunkwan University, Suwon 440-746, South Korea

⁴Department of Physics and Department of Chemistry and Nano Science, Ewha Womans University, Seoul 120-750, South Korea

(Received 18 November 2010; accepted 29 December 2010; published online 18 January 2011)

A radial heterojunction nanowire diode (RND) array consisting of a ZnO (shell)/Si (core) structure was fabricated using conformal coating of a n -type ZnO layer that surrounded a p -type Si nanowire. In both ultraviolet (UV) and visible ranges, the photoresponsivity of the RND was larger than that of a planar thin film diode (PD) owing to the efficient carrier collection with improved light absorption. Compared to a PD, in the forward bias, a 6 μm long RND resulted in a ~ 2.7 times enhancement of the UV responsivity at $\lambda = 365$ nm, which could be explained based on the oxygen-related hole-trap mechanism. Under a reverse bias, UV-blind visible detection was observed while the UV response was suppressed. © 2011 American Institute of Physics.

[doi:10.1063/1.3543845]

One-dimensional semiconductor nanowires (NWs) have attracted much attention for use in optoelectronic applications due to their unique optical and electrical properties.¹⁻³ In particular, ZnO NWs are considered a promising material for light-emitting diodes, laser diodes, and photodetectors because ZnO NWs have a wide band gap (3.37 eV), large exciton binding energy (60 meV), and a high photoconductivity gain.³ Since several key issues⁴ such as deep acceptor levels and low dopant solubilities have prevented reproducible fabrication of p -type ZnO for p - n homojunctions, n -ZnO/ p -Si heterojunctions have been intensively investigated as an alternative approach.⁵⁻⁷

Heterojunction photodiodes demonstrate UV and visible photoresponses due to the large band offset at the interface with the significant difference in the band gaps of ZnO and Si. Mridha and Basak⁶ demonstrated that n -ZnO/ p -Si thin film photodiodes could selectively detect either UV or visible photons by varying the applied bias. Although ZnO or Si NW structures have been introduced in previous studies^{7,8} to obtain a high conductivity gain with a ZnO NW or strong light absorption with a Si NW, the entire NW surface has not been used as a junction region due to insufficient conformal deposition.

In this study, we demonstrate radial heterojunction NW photodiodes (RNDs) consisting of p -Si/ n -ZnO NW core/shell structures which were fabricated using atomic layer deposition (ALD). Their photoresponse properties are anticipated to provide insight for the formation of promising photodetector nanodevices. Conformal coating with a thin ZnO layer formed a depletion region on a several microns long Si NW across the entire interface area. The RND exhibited enhanced UV and visible responsivities compared to a planar

thin film photodiode (PD). The photoresponse selectivity of a RND in the visible to UV range was found to be significantly enhanced compared to a PD. All of the experimental data can be understood based on the unique advantages of the RND geometry.

Figure 1(a) illustrates the configuration used for the photoresponse measurements of a RND. Vertically dense Si NW arrays were fabricated by Ag-induced electroless etching of p -type Si wafers (resistivity of 1–10 Ωcm).⁹ The NW length could be easily controlled by varying the etching time. After formation of the Si NW arrays, the ALD technique was used to conformally coat a n -type ZnO thin film on the high aspect ratio Si NWs.¹⁰ A 100 nm thick ZnO layer was depos-

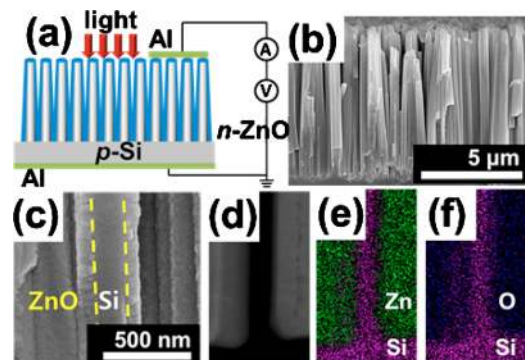


FIG. 1. (Color online) (a) Schematic showing the configuration of the photoresponse measurement system used for the n -ZnO(shell)/ p -Si(core) radial nanowire photodiodes. (b) A typical cross-sectional SEM image of the n -ZnO/ p -Si NW arrays. (c) A magnified image showing the bottom region of a ZnO/Si NW, in which the ZnO shells were partly peeled off during the sample preparation. A uniform thickness of ZnO over the Si core is observed. The yellow dashed lines indicate the position of the interface between ZnO and Si. (d) A scanning TEM image with [(e) and (f)] two-dimensional energy dispersive x-ray spectroscopy mapping of Zn (green), O (white), and Si (purple).

^{a)}Authors to whom correspondence should be addressed. Electronic addresses: dwkim@ewha.ac.kr and jungho@hanyang.ac.kr.

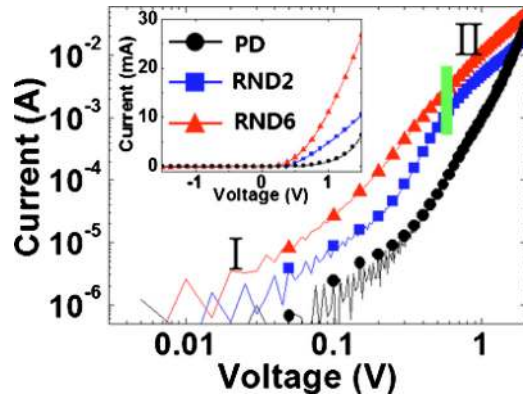


FIG. 2. (Color online) Logarithmic I - V plots of the RNDs and PD. For the RNDs, “I” and “II” refer to the regions dominated by the different transport behaviors with the applied bias. Linear I - V plots are also shown in the inset.

ited at 150 °C to form the n -ZnO/ p -Si NW junctions. The standard resistivity and carrier concentration were measured to be $4.6 \times 10^{-3} \Omega \text{ cm}$ and $5.1 \times 10^{19} \text{ cm}^{-3}$, respectively, on ZnO thin films deposited under identical conditions on glass substrates. Top and bottom electrodes were formed using 250 nm thick Al thin films which were evaporated both on the front (ZnO) and substrate backside. The properties of long (6 μm) and short (2 μm) nanowire photodiodes, denoted as RND2 and RND6, respectively, were compared to a PD. The aspect ratios of the RNDs, which were calculated using the averaged values of the lengths and diameters, were ~ 10 and 30 for RND2 and RND6, respectively.

The typical diameter of the n -ZnO/ p -Si NW arrays was 350–400 nm, which consisted of a 100 nm thick shell and a 150–200 nm thick NW core [Figs. 1(b) and 1(c)]. All of the ZnO/Si heterojunction devices exhibited nonlinear rectifying behaviors in their I - V characteristics (inset in Fig. 2) but the overall measured current levels under forward and reverse biases were higher in the RNDs than in the PD due to the increased junction area. The presence of interface states is also known to increase the reverse current, i.e., leakage current.^{6,7} Further analysis of the logarithmic plots (Fig. 2) of the I - V data suggests a clear difference between the transport behaviors of the RNDs and PD. The forward bias current exponentially increased in the PD according to the relationship of $I \propto \exp(\alpha V)$ due to the recombination-tunneling mechanism⁷ in the wide band gap p - n heterojunction. On the other hand, two different regions depending on the bias level were observed in the RNDs.

For the very low bias range (region I) of $0 < V < 0.8$ V, almost the same rectifying behavior as a PD was observed with the RNDs due to the recombination-tunneling mechanism. However, the I - V behavior normally followed the relationship of $I \propto (V - V_0)^2$ for the high bias range of $V > 0.8$ V (region II). This may be attributed to the space-charge-limited current (SCLC) conduction, which has often been observed in semiconductor nanostructures including thin films.⁷ The SCLC effect was reported¹¹ to be greatly amplified in cases using NWs, in which inherent geometrical and material issues such as poor electrostatic screening in high-aspect ratio structures, enhanced carrier depletion due to surface states, and charge traps incorporated during the nanostructure growth are influential. The higher levels of the reverse current and SCLC conduction observed in the RNDs

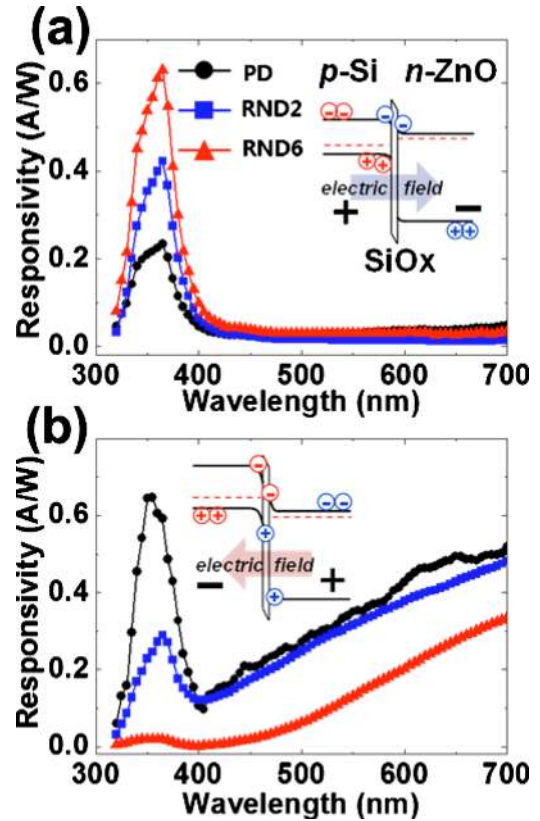


FIG. 3. (Color online) Photoresponsivity spectra of the RNDs and PD measured under (a) forward and (b) reverse biases. Their energy band diagrams and charge transport mechanisms are also depicted in the insets.

corroborate the notion that the increased ZnO/Si interfacial area mostly operated as radial heterojunctions.

The energy band diagrams of the ZnO/Si heterojunction under forward and reverse biases are depicted in the insets of Figs. 3(a) and 3(b), respectively. Given the band gaps and electron affinities of ZnO and Si,⁵ a valence band offset (2.55 eV) greater than the conduction band offset (0.4 eV) is expected for a n -ZnO/ p -Si heterojunction. Figure 3(a) shows the photoresponsivity spectra under a forward bias of 0.5 V. Since the transmittance of ZnO on a glass substrate was measured to be over 80% in the visible range (400–700 nm), visible light is normally absorbed in the underlying p -Si after passing through the ZnO layer. The absorbed light generates electron-hole pairs (EHP) inside the Si. The electric field drives the photogenerated holes toward the n -ZnO side, but they cannot cross over the SiO_2 layer between p -Si and n -ZnO due to the high potential barrier for holes, as shown in the inset of Fig. 3(a). Thus, the visible photoresponsivity is mainly attributed to the transport of photogenerated electrons (minority carriers) in p -Si, which is very low in magnitude. The photoresponsivity remained nearly constant in the visible range (400–700 nm) for all samples.

In contrast with the response to visible light, the photoresponsivity spectra with UV exposure showed a strong response under a forward bias. Since the penetration depth of UV light is less than 100 nm in ZnO, most photons from the UV light are absorbed in the ZnO layer. The strong UV response can be explained by the different drift behaviors of the electrons (photogenerated in ZnO) and holes (photogenerated in Si). The electrons photogenerated in ZnO can easily move to Si due to the relatively low potential barrier at

the interfacial region while the photoholes in Si cannot tunnel through the high potential barrier.^{5,6}

In addition, the UV responsivities of RND2 and RND6 are higher than that of the PD under a forward bias. Soci *et al.*³ reported that the enhanced UV photoconductive response in ZnO NWs could be attributed to the presence of oxygen-related hole-trap states at the NW surface. The trap states can prolong the photocarrier lifetime while preventing charge-carrier recombination (hole-trapping mechanism). Photoholes are readily trapped by the negatively charged oxygen ions, leaving behind unpaired electrons which are either collected at the electrode or recombine with holes. As a result, RNDs can improve the UV photodetection sensitivity due to the high surface area to volume ratio. Figure 3(a) confirms that the forward bias UV responsivity was improved by increasing the NW length (increased surface area to volume ratio), in which the UV responsivities at $\lambda=365$ nm were detected to be 0.23, 0.42, and 0.63 A/W for PD, RND2, and RND6, respectively. In the wavelength range of 300–365 nm, the UV responsivities drastically decreased with decreasing wavelength since the penetration of high energy photons became very short (<40 nm).⁵ Due to the short penetration depth, the carrier generation normally occurs near the surface. Significant surface scattering and recombination decrease the carrier lifetime.

Note that the UV photoresponse of RNDs under a reverse bias shown in Fig. 3(b) is significantly suppressed compared to the PD. The visible/UV responsivity ratios calculated using the responsivities measured at $\lambda=700$ and 365 nm were 17.2 for RND6 and 0.86 for PD. A previous work³ reported that the ZnO surface can be depleted by the surface oxygen absorption according to the hole-trapping mechanism. For the forward bias, carrier depletion behavior at the NW surface is beneficial for photoelectrons to transport from ZnO to Si via the effective carrier separation. Under a reverse bias, however, the surface depletion of ZnO acts as a diffusion barrier for photoelectrons to collect at the top electrodes. This feature causes the electrons to suffer from serious recombination, which finally results in a remarkable suppression of the UV photoresponse with increasing NW length.

In contrast with the forward bias, a monotonous increase with increasing wavelength was observed in the visible response results (400–700 nm) under a reverse bias. The incident visible light can generate EHPs in the *p*-Si layer where the photogenerated electrons and holes under the reverse bias move to the ZnO and Si sides, respectively. The radial heterojunction geometry is known to help efficient carrier collection and light trapping.^{1,2} Contrary to the expectation, the visible photoresponsivities of the RNDs were observed to be similar to or even lower than that of the PD. This can be explained by the morphology of the highly dense ZnO/Si NW arrays. The ZnO thickness normally increases closer to

the NW bottom region due to overlaying of the ZnO shells via merging of adjacent wires during ZnO deposition, as shown in Figs. 1(a) and 1(b). Increasing the ZnO thickness at the NW bottom degrades the visible transmittance,¹² which results in the inferior light absorption in Si. Given that a similar visible responsivity to the PD was observed in RND2, the actual responsivity of the RND, which has a thicker ZnO layer at the NW bottom under the same coating condition, is also estimated to be higher than that of the planar counterpart.

In conclusion, we fabricated *n*-ZnO/*p*-Si RNDs using metal-assisted electroless etching of Si and conformal coating of ZnO by an ALD process. Compared to a planar ZnO/Si heterojunction, both the UV and visible photoresponsivities of the RNDs were enhanced, owing to the enlarged surface area to volume ratio, efficient carrier collection, and improved light absorption. In addition, our RNDs exhibited either UV-blind visible or visible-blind UV photoresponse, depending on the bias polarity. All of the advantageous characteristics of the RNDs can be further improved by optimizing the device design and fabrication processes.

This work was supported by the Pioneer Research Center Program (Grant No. 2010-0002231) and Nano R&D Program (Grant No. 20090083229) through the National Research Foundation grant funded by the Ministry of Education, Science and Technology. This work was supported by the New and Renewable Energy of the Korea Institute of Energy Technology Evaluation and Planning grant funded by the Ministry of Knowledge Economy (Grant No. 2009T100100614). H.-D.U., K.-T.P., and S.-W.J. acknowledge financial support of the fifth-stage Brain Korea 21 Project in 2010.

¹B. M. Kayes, H. A. Atwater, and N. S. Lewis, *J. Appl. Phys.* **97**, 114302 (2005).

²E. Garnett and P. Yang, *Nano Lett.* **10**, 1082 (2010).

³C. Soci, A. Zhang, B. Xiang, S. A. Dayeh, D. P. R. Aplin, J. Park, X. Y. Bao, Y. H. Lo, and D. Wang, *Nano Lett.* **7**, 1003 (2007).

⁴Y. Ma, G. T. Du, S. R. Yang, Z. T. Li, B. J. Zhao, X. T. Yang, T. P. Yang, Y. T. Zhang, and D. L. Liu, *J. Appl. Phys.* **95**, 6268 (2004).

⁵I.-S. Jeong, J. H. Kim, and S. Im, *Appl. Phys. Lett.* **83**, 2946 (2003).

⁶S. Mridha and D. Basak, *J. Appl. Phys.* **101**, 083102 (2007).

⁷S. Y. Liu, T. Chen, Y. L. Jiang, G. P. Ru, and X. P. Qu, *J. Appl. Phys.* **105**, 114504 (2009).

⁸C. Y. Huang, Y. J. Yang, J. Y. Chen, C. H. Wang, Y. F. Chen, L. S. Hong, C. S. Liu, and C. Y. Wu, *Appl. Phys. Lett.* **97**, 013503 (2010).

⁹H. D. Um, J. Y. Jung, H. S. Seo, K. T. Park, S. W. Jee, S. A. Moiz, and J.-H. Lee, *Jpn. J. Appl. Phys., Part 1* **49**, 04DN02 (2010).

¹⁰B. H. Kong, M. K. Choi, H. K. Cho, J. H. Kim, S. Baek, and J.-H. Lee, *Electrochem. Solid-State Lett.* **13**, K12 (2010).

¹¹A. A. Talin, F. Léonard, B. S. Swartzentruber, X. Wang, and S. D. Hersee, *Phys. Rev. Lett.* **101**, 076802 (2008).

¹²X. Yu, J. Ma, F. Ji, Y. Wang, C. Cheng, and H. Ma, *Appl. Surf. Sci.* **245**, 310 (2005).